Check for updates

Bioelectromagnetics 42:212–223 (2021)

Effects Induced by a Weak Static Magnetic Field of Different Intensities on HT-1080 Fibrosarcoma Cells

Hakki Gurhan,[1]* Rodolfo Bruzon,[1] Sahithi Kandala,[1] Ben Greenebaum,[2] and Frank Barnes[1]

[1]Department of Electrical, Computer and Energy, University of Colorado Boulder, Boulder, Colorado

[2]Department of Physics, University of Wisconsin-Parkside, Kenosha, Wisconsin

In this study, we investigated the effects of weak static magnetic fields (SMFs) on HT-1080 human fibrosarcoma cells. Exposures to SMFs for four consecutive days were varied from 0.5 to 600 μT for treated units, while exposures to control units were held at 45 μT. Growth rates were measured by comparing cell counts, whereas membrane potentials, mitochondrial calcium, mitochondrial superoxide (O_2^-), nitric oxide (NO), hydrogen peroxide (H_2O_2), intercellular pH, and oxidative stress were measured by using fluorescent dyes. The relative cell growth rates vary with the angle of the SMFs. Increases in the magnitude of the SMFs increased concentrations of mitochondrial calcium and membrane potential and decreased intracellular pH. H_2O_2, an important reactive oxygen species (ROS), increases at 100 and 200 μT, decreases at 300 and 400 μT and increases again at 500 and 600 μT. Overall, oxidative stress increases slightly with increasing SMFs, while superoxide and NO concentrations decrease. These results indicate that weak SMFs can accelerate and inhibit cell growth rates and induce alterations in ROS. Changes in ROS and oxidative stress are important for various cell functions. Calcium influx into mitochondria was one of the initial steps into the corresponding changes. Bioelectromagnetics. 2021;42:212–223. © 2021 Bioelectromagnetics Society

Keywords: **cell growth; membrane potential; oxidative stress; reactive oxygen species; weak static magnetic field**

INTRODUCTION

In recent years, the biological effects of static magnetic fields (SMFs) have attracted increased interest. An objective of the work being reported in this paper is to provide data on the effects of SMFs on the growth rates of fibrosarcoma cells and also on some of the chemistry important to part of the communications systems both within and between cells. In reporting some of the effects of changes in SMFs on changes in HT-1080 cancer cell growth rates, we also report changes in signaling molecules and other cell parameters, including membrane potentials, intracellular pH, nitric oxide (NO), mitochondrial calcium, oxidative stress, and reactive oxygen species (ROS) such as superoxide (O_2^-) and hydrogen peroxide (H_2O_2), to help improve our understanding of the mechanisms by which magnetic fields (MFs) are modifying the growth rates. This information will be useful in further studies using MFs as a tool for modifying biological systems, for medical applications, and for understanding possible safety implications of long-term low-level exposure to electromagnetic fields, such as man-made SMFs generated by home appliances, transmission lines, and electric appliances, which are capable of producing MFs between 0.01 and 167 μT [Greenebaum and Mild, 2018].

Relatively recently, weak SMFs have been shown to modify the concentrations of ROS. ROS are useful as signaling molecules in mammalians but also cause cellular damage if produced in an uncontrolled manner

Grant sponsors: National Science Foundation (NSF), grant number: award #CBET 1644371; Milheim Foundation; DARPA, grant number: HR00111810006.

Conflicts of interest: None.

*Correspondence to: Hakki Gurhan, Department of Electrical, Computer and Energy, University of Colorado Boulder, 425 UCB #1B55, Boulder, CO 80309.
E-mail: hakki.gurhan@colorado.edu

Received for review 22 April 2020; Revised 20 February 2021; Accepted 3 March 2021

DOI:10.1002/bem.22332
Published online 18 March 2021 in Wiley Online Library (wileyonlinelibrary.com).

© 2021 Bioelectromagnetics Society

[Hancock et al., 2001]. There are several sources of ROS in cells, including extracellular ROS, generation of ROS at the plasma membrane, and mitochondrial ROS [Vriz et al., 2014; Zhang et al., 2016; Diwanji and Bergmann, 2018; Moloney and Cotter, 2018]. It is estimated 1%–2% of the cell′s oxygen consumption is converted into ROS and the level of ROS production is essential for the physiological control of a variety of cell functions [Turrens, 2003]. ROS also have long been associated with cancer [Reczek and Chandel, 2017]. Compared with normal cells, cancer cells have an altered redox environment, with a high rate of ROS production counterbalanced by a high rate of ROS scavenging. This unique characteristic of cancer cells may make them more sensitive than normal cells to alterations in ROS levels or redox manipulations [Gorrini et al., 2013]. Various results show that SMFs are able to induce alterations in ROS production, antioxidant response, and mitochondrial balance [Sullivan et al., 2011; Jouni et al., 2013; Van Huizen et al., 2019; Novikov et al., 2020]. Controlling mitochondrial ROS production in cancer cells can be exploited for therapeutic benefits. Therefore, we looked at ROS changes in human fibrosarcoma cancer cell line HT-1080 to observe such effects under the exposure of external weak SMFs.

At the time this study was initiated, it was not widely recognized that taking care of the presence or absence of weak SMFs other than the natural earth′s magnetic field was important if one were to obtain reproducible results, even though it had been reported in a number of papers [Liboff, 2007; Portelli et al., 2013]. Additionally, both the acceleration and inhibition of cell growth rates are expected as a result of changing both frequency and the amplitude of the applied electromagnetic fields [Bingham, 1996]. An increasing number of studies suggested that short- and long-term exposure to MFs can affect oxidative stress and induce downstream biological effects. The induced biological effects depend on the characteristics of the MF exposure, duration of exposure, and relation to the status of the oxidative stress and antioxidant defense system in the organism, due to the cells being in different growth life stages. A review of many of the effects of MFs on oxidative stress is presented by Wang and Zhang [2017], and long-term increases in oxidative stress are associated with cancer, aging, and Alzheimer′s disease [Droge, 2002].

The influx of Ca^{2+} through the plasma membrane is possibly the main mechanism for many of the effects of SMFs. For many years, attention has focused on the role of Ca^{2+} as an initiator of the biological effect induced by SMF. Now we know that enhanced Ca^{2+} transport through Ca^{2+} channels, as well as the inhibition of Ca^{2+} pumps, occur in the presence of oxidants. The influx of calcium through the plasma and mitochondrial membrane can be associated with the activation of voltage-dependent calcium channels by the SMF [Prina-Mello et al., 2005]. Many of the reported effects of moderate SMF can be explained on the basis of alterations in membrane calcium influx [Fanelli et al., 1999; Belton et al., 2008; Morris and Skalak, 2008]. Surma et al. [2014] showed that an SMF in the range of 60–400 μT induces a 1.5- to 3.5-fold rise in the concentration of intracellular calcium due to the release of calcium from the sarcoplasmic reticulum through ryanodine receptors. Exposure to SMF (2 mT) is immediately (about 1 min) followed by a reversible cell membrane depolarization wave that causes the rise of intracellular calcium and the decrease of mitochondrial activity of vital granulosa cells [Bernabò et al., 2014]. Kim et al. [2015] reported that SMFs (3–50 mT) increased cell proliferation, alkaline phosphatase activity, calcium release, and mineralized nodule formation in a dose- and time-dependent manner, which peaked at 15 mT. Calabrò et al. [2013] found that an SMF of 2.2 mT produced a decrease of mitochondrial potential up to 30% in SH-SY5Y cells after 24 h of exposure. The effect was associated with ROS production increase.

MFs have been shown to change radical concentrations [Batchelor et al., 1993; Grissom, 1995; Hayashi, 2004; Timmel and Henbest, 2004]. Spin modulation in the radical pair recombination mechanism is considered a plausible explanation of how the SMF can alter the chemistry of reactions and cause biological effects [Barnes and Greenebaum, 2015]. The radical pair mechanism is used to exemplify how applied MFs weaker in strength than typical hyperfine interactions can influence the yields and kinetics of recombination reactions of free radicals in solution [Timmel et al., 1998]. Short-term changes in radical concentrations are important signaling mechanisms [Antunes and Cadenas, 2000]. Long-term departures from their normal ranges can lead to biological damage that is associated with cancer, aging, and Alzheimer′s disease [Droge, 2002; Ghodbane et al., 2013].

In this study, we identify some of the effects in cell physiology due to weak SMF exposure on HT-1080 fibrosarcoma cells. This includes increasing our understanding of how these fields signal changes in some of the chemical reaction rates while also modifying the growth rates of growing cells. We report changes in a variety of cell parameters by modifying the field strength and angle of the SMFs while controlling the external environment.

1521186x, 2021, 3, Downloaded from https://onlinelibrary.wiley.com/doi/10.1002/bem.22332 by University Of Colorado Libraries, Wiley Online Library on [30/05/2024]. See the Terms and Conditions (https://onlinelibrary.wiley.com/terms-and-conditions) on Wiley Online Library for rules of use; OA articles are governed by the applicable Creative Commons License

MATERIALS AND METHODS

Cell Culture

Human fibrosarcoma HT-1080 cells (ATCC CCL-121, Manassas, VA) were grown on Eagle′s minimum essential medium (EMEM) (ATCC 30-2003) supplemented with 10% fetal bovine serum (FBS) (ATCC 30-2020). The cells were cultured in treated flasks of 75 cm^2 (229341; Celltreat, Pepperell, MA) to expand cell numbers. After reaching a confluence between 70% and 90%, the cells were seeded in other flasks or culture plates, depending on the type of experiment. Cells were maintained under controlled conditions of temperature (37 °C), CO_2 concentration (5%), and relative humidity (90%).

SMF Stimulation

The experiments were carried out in a Forma Scientific (Model 3325, Marietta, OH) water-jacketed incubator containing a pair of Mu-metal shields (The MuShield Company, Manchester, NH) and two sets of Helmholtz coils so that we could control the SMF and obtain reproducible conditions (Fig. 1). One set of coils was activated for the exposed cultures, and the other served the controls. The data were processed without knowing whether it was obtained from control or exposed, reducing the potential for bias. Reduction of background MF was achieved by using Mu-metal boxes (The MuShield Company). 0.5 μT is the lowest SMF we can achieve without additional shielding.

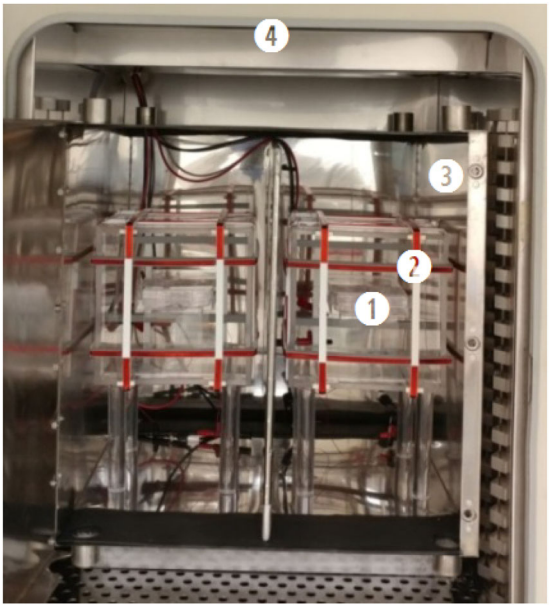


Fig. 1. Magnetic system formed tri-axial square Helmholtz. (**1**) Flask with fibrosarcoma cells. (**2**) Helmholtz coils. (**3**) Mu-metal chamber. (**4**) CO_2 incubator.

MFs were formed either by tri-axial square Helmholtz coils that allowed us to generate uniform MFs at 45° (Fig. 1) or by 1-axis coils to apply fields of various intensities either in the vertical or horizontal direction with respect to the plate. The control cells in the exposure chamber were maintained with an MF of 45 μT, and their other parameters such as humidity, carbon dioxide, and temperature were identical to those of the cells exposed to the different values of MFs.

The windings of the Helmholtz coils were made of 1.63 mm wire to overcome heating problems and to keep the cells′ temperature close to 37 °C. The dimensions of the coils (side = 15 cm) were chosen taking into consideration the size of the culture flask. The measurements of the MF were made using the fluxgate magnetometer FGM-4D2N with a resolution of 1 nT (Walker Scientific, Worcester, MA). The homogeneity of the exposure fields varied ±5% across the region where culture plates were placed. We applied a voltage of 6 mV to generate a field of 45 μT. The electric field between the pair of Helmholtz coils is approximately 1.5 mV/m; the electric field seen by the cells is less than this due to the Mu-metal shields and distance and scales with the current and the MF.

Temperature Control

The temperature was continuously monitored during the performance of the experiments. We used the NI 9211 type T thermocouple input module with the auto-zero channel on, measurement sensitivity = 0.07 °C, and data acquisition software LabVIEW, Version 16.0, both developed by National Instruments (Austin, TX). We also used the USB-TC model with measurement sensitivity = 0.04 °C and data acquisition software DAQami, Version 4.2, both developed by Measurement Computing (Contoocook, NH).

Table 1 shows the values of the MF and the temperature under which the different experiments were performed. The temperature of the controls was adjusted to match the slight heating of exposed cultures at higher fields due to current in the Helmholtz coils. We studied the effect of temperature on cell growth under continuous exposure at 45 μT. We did not observe significant differences in cell growth between 36° and 38° after 4 days of treatment at 45 μT (Fig. 2).

One of the most important things is to get an even cell suspension. To prevent cells from gathering at the center of the wells or flasks, the cell suspension was added by pipettes to the bottom of the wells or flasks. After adding the cell suspension to the wells or flasks, several figure-8-shaped shaking movements

1521186x, 2021, 3, Downloaded from https://onlinelibrary.wiley.com/doi/10.1002/bem.22332 by University Of Colorado Libraries, Wiley Online Library on [30/05/2024]. See the Terms and Conditions (https://onlinelibrary.wiley.com/terms-and-conditions) on Wiley Online Library for rules of use; OA articles are governed by the applicable Creative Commons License

TABLE 1. Values of the Magnetic Field and the Temperature in the Different Experiments

Experiments	Treated group, B (μT) ⇔ T (°C)	Control group, B (μT) ⇔ T (°C)	ΔT (°C)
I	0.5 ⇔ 36.94	0.5 ⇔ 36.94	0
II	45 ⇔ 36.96	0.72 ⇔ 36.94	0.02
III	100 ⇔ 37.09	45 ⇔ 37.03	0.06
IV	200 ⇔ 37.15	45 ⇔ 37.06	0.09
V	300 ⇔ 37.17	45 ⇔ 37.08	0.09
VI	400 ⇔ 37.25	45 ⇔ 37.11	0.14
VII	500 ⇔ 37.38	45 ⇔ 37.15	0.23
VIII	600 ⇔ 37.45	45 ⇔ 37.16	0.29

spread the cells more evenly. In addition, we allowed the plates and flasks to sit for 3–5 min so that cells settled to the bottom before being placed in the incubators.

Cell Growth Studies

For cell growth experiments, HT-1080 fibrosarcoma cells were cultured in cell culture flasks (430639; Corning, Corning, NY) (surface area 25 cm^2). Experiments used cell culture passages between 3 and 12 to prevent genomic abnormalities. For the cell counting assay, four flasks were seeded at a concentration of 11×10^4 cells per flask and incubated in 5% CO_2 at 37 °C. Depending on the type of experiment, one or two flasks were taken from the incubator every 24 h and the following protocol was followed. The culture medium was removed and the cells washed with phosphate-buffered saline (PBS) (4 ml per flask). PBS was removed and 1 ml of trypsin was added per flask. The cells were placed in the incubator for 4 min at 37 °C. The culture flask was observed under a microscope to verify that the cells had detached from the bottom. Trypsin was neutralized by adding 5 ml of medium per flask. The solution was placed in a centrifuge tube and centrifuged at 1000 rpm for 6 min using the Premiere Centrifuge XC-2000 (C&A Scientific, Sterling, VA). The supernatant was removed and 1 ml of culture medium was added and gently mixed using a pipette to obtain a homogenous cell suspension. Sixty microliters of the cell suspension and 60 μl of trypan blue were added and mixed gently several times. For each individual count, 10 μl was used.

As it takes 4 days for cells to reach confluence between 70% and 90%, the MF was continuously applied for 4 days for both controls and treated units during the experiments. The effect of magnetic treatment on cell growth was determined by counting cell numbers after 2, 3, and 4 days of stimulation for different experiments. In this case, we used eight flasks, four for the samples treated with varying MFs (SMF = 0.5, 100, 200, 300, 400, 500, and 600 μT) and four taken as controls, which were exposed to 45 μT SMF. Cell growth studies were performed using the Countess II Automated Cell Counter (Thermo Fisher Scientific, Waltham, MA). Detection time was approximately 12 min in each experiment for measuring cell counts of both treated and control units. Cells had been diluted 1:1 in trypan blue, and the Cell Counter used this dilution to calculate the total cell concentration. The cell concentration displayed on the screen appears directly in cells/ml. Four samples were taken in each experiment, and we have a total of 12 samples as each cell growth experiment was run in triplicate. For each experimental condition, the mean and standard deviation corresponding to 12 measurements are presented.

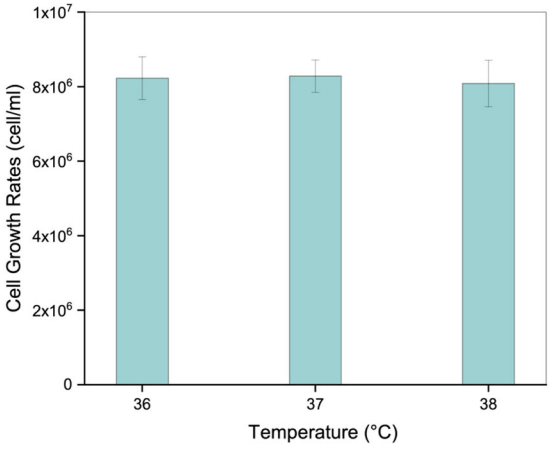


Fig. 2. Cell growth rates as a function of temperature under continuous exposure at 45 μT. The data are expressed as mean ± SD; $n = 12$ for each group.

Fluorescence Studies

Fluorescent assay measurements were made by using 9 wells in a 12-well plate (229111; Celltreat, Pepperell, MA) (surface area per well 3.85 cm^2). In the experiments, 18 wells in two plates were seeded at a concentration of 19,250 cells per well and incubated in 5% CO_2 at 37 °C; 1 ml of the cell suspension was put into each well. Nine wells were treated with varying MFs (SMF = 0.5, 100, 200, 300, 400, 500, and 600 μT) and nine taken as controls which were exposed to 45 μT SMF. Similar to cell growth studies, the MF was continuously applied for four days for both controls and treated units during the experiments. The protocol followed in the sample preparation was similar to that used in cell growth studies. Fluorescence studies were performed after the fourth day of

1521186x, 2021, 3, Downloaded from https://onlinelibrary.wiley.com/doi/10.1002/bem.22332 by University Of Colorado Libraries, Wiley Online Library on [30/05/2024]. See the Terms and Conditions (https://onlinelibrary.wiley.com/terms-and-conditions) on Wiley Online Library for rules of use; OA articles are governed by the applicable Creative Commons License

continuous exposure to SMF using a multi-detection microplate reader, Synergy HT (BioTek Instruments, Winooski, VT). Detection time was approximately 8 min in each experiment for measuring densities of both treated and control units. The effect induced by SMF was examined for three different parameters. Three wells were used per parameter and in each well 21 measurements were made, so that each fluorescence experiment was run in triplicate. As a result, we have a total of 63 measurements per parameter, and therefore for each experimental condition, the mean and standard deviation corresponding to 63 measurements are presented.

Membrane potential. Twelve microliters of FluoVolt (Thermo Fisher Scientific) dye, 1000× and 120 µl 100× PowerLoad concentrate, and 12 ml PBS were added into a 15-ml tube and mixed to prepare fresh FluoVolt Loading Solution. Medium from adherent cells was removed and cells were washed twice in PBS. One microliter of FluoVolt Loading Solution was added to each well containing cells, the cells were incubated at room temperature for 30 min before fluorescence measurements were taken, and FluoVolt Loading Solution cells were washed twice and suspended in PBS. The fluorescence intensity from these cells was measured using a Synergy HT fluorescence plate reader (BioTek Instruments) with appropriate wavelength settings (excitation at 522 nm, emission at 535 nm).

Mitochondrial calcium. The Rhod-2 AM (Thermo Fisher Scientific) probe was used to determine mitochondrial Ca^{2+} level in HT-1080 human fibrosarcoma cells. Cells were washed and suspended in PBS containing Rhod2-AM (1 µM). Cells were normally incubated with the AM ester for 30 min at 37 °C. Before fluorescence measurements were taken, the cells were washed and suspended in PBS. The fluorescence intensity from these cells was measured using the fluorescence plate reader with appropriate wavelength settings (excitation at 550 nm, emission at 580 nm).

Intracellular pH. For intracellular pH measurements, pHrodo Green AM Intracellular pH Indicator (Thermo Fisher Scientific) was used. Ten microliters of pHrodo Green AM was mixed with 100 µl of PowerLoad concentrate, and this dye solution was then diluted with 10 ml PBS. The growth medium was removed from cells, which were then washed once with PBS. The mixture of pHrodo Green AM/PowerLoad/PBS was added to cells, followed by incubation at 37 °C for 30 min. Then, cells were analyzed in the fluorescence plate reader using an excitation maximum at 509 nm and emission maximum at 533 nm.

Oxidative stress. SMF-induced oxidative stress was determined using CellROX Green reagent for oxidative stress detection (Life Technologies, Carlsbad, CA). HT-1080 human fibrosarcoma cells were stained with 5 µM of CellROX Green reagent by adding the probe to the complete medium and incubating cells at 37 °C for 30 min. The cells were then washed, suspended with PBS, and analyzed on a fluorescence plate reader with appropriate wavelength settings (excitation at 485 nm, emission at 520 nm).

Hydrogen peroxide. Amplex Red reagent (Invitrogen, Carlsbad, CA) assay was used to measure the production of H_2O_2 in HT-1080 fibrosarcoma cells. The contents of the vial of the Amplex Red reagent were dissolved in 60 µl of dimethylsulfoxide (DMSO) to make a 10 mM Amplex Red reagent stock solution. Four microliters of 5× reaction buffer was added to 16 ml deionized water to make a 1× reaction buffer solution. The contents of the vial horseradish peroxidase (HRP) were dissolved in 1.0 ml of 1× reaction buffer to make a 10 U/ml HRP stock solution. Fifty microliters of 10 mM Amplex Red reagent stock solution, 100 µl of 10 U/ml HRP solution, and 4.85 ml of 1× reaction buffer were mixed. Five hundred microliters of the Amplex Red reagent/HRP working solution was added to each microplate well. Reactions were incubated at room temperature for 30 min, and fluorescence was measured for an excitation maximum at 571 nm and emission maximum at 585 nm.

Mitochondrial superoxide. We used a fluorescent probe (MitoSOX Red reagent) (Thermo Fisher Scientific) that specifically detects superoxide within the mitochondrial matrix. The contents (50 mg) of one vial of MitoSOX mitochondrial superoxide indicator were diluted in 13 µl of DMSO to make a 5 mM MitoSOX reagent solution. The 5 mM MitoSOX reagent solution was diluted in PBS to make a 5 µM MitoSOX reagent working solution. Cells were washed and suspended in PBS containing the 5 µM MitoSOX reagent working solution. Afterward, cells were incubated for 10 min at 37 °C. The fluorescence intensity from these cells was measured using the fluorescence plate reader with appropriate wavelength settings (excitation at 510 nm, emission at 580 nm).

Nitric Oxide. Intracellular NO level was measured using a DAF-FM diacetate NO indicator (D23844; Invitrogen). A 5 mM stock solution of DAF-FM diacetate was made by dissolving 50 mg packaged

1521186x, 2021, 3, Downloaded from https://onlinelibrary.wiley.com/doi/10.1002/bem.22332 by University Of Colorado Libraries, Wiley Online Library on [30/05/2024]. See the Terms and Conditions (https://onlinelibrary.wiley.com/terms-and-conditions) on Wiley Online Library for rules of use; OA articles are governed by the applicable Creative Commons License

DAF-FM diacetate (D-23844) in a 20 µl of DMSO. The DMSO stock solution was diluted in PBS to a 1 µM final concentration. HT-1080 human fibrosarcoma cells were incubated with the diluted DAF-FM diacetate for 30 min at 37 °C. Then, cells were washed with PBS to remove the excess probe and replaced with fresh PBS. The fluorescence intensity from those cells was measured using the fluorescence plate reader with appropriate wavelength settings (excitation at 495 nm, emission at 515 nm).

Statistical Analysis

Differences in cell growth rates and fluorescence were considered statistically significant for $P < 0.05$. Comparison of two independent samples used the Student′s *t* test. The one-way analysis of variance test was used to contrast the means of multiple independent samples. We used the Tukey posthoc test to indicate which groups were significantly different with respect to the control. Data are expressed as mean ± standard deviation. In Figures 3–13, * indicates significance level at $P < 0.05$; ** significance level at $P < 0.01$, and *** significance level at $P < 0.001$. For normalization, each of the experimental groups was compared to its corresponding control group, held at 45 µT, the nominal earth′s MF. For the statistical analysis of the data, we used the software Origin Pro 2017 Statistical Package (OriginLab, Northampton, MA).

RESULTS

In Figures 3 through 13, we show the results from exposing HT-1080 fibrosarcoma cells to different intensities of SMFs. Cells are exposed to SMF in the range from 0.5 to 600 µT for a period of 4 days each.

Changes in Cell Growth With Changes in SMFs

Cell growth is a critical feature of cell cycle entry and refers to cell division and increase in cell quantity. The environment in which cells live plays an important role in modifying the rate and extent of growth. Figure 3 shows the changes in growth rates when HT-1080 cells were exposed to SMF in the range from 0.5 to 600 µT for a period of four days. Growth rates increase from 0.5 to 400 µT and then decrease to 600 µT. It is to be noted the growth rates at 0.5 and 600 µT are 9% ($P < 0.001$) less than the growth rate at 45 µT (Control), which is approximately equal to the earth′s magnetic field in Boulder, Colorado. The growth rates at 300 and 400 µT exceed the growth rate at 45 µT by 23% ($P < 0.001$) and 28% ($P < 0.001$), respectively. In addition to observing SMF effects at the end of the 4 days of exposure, we also measured cell growth curves for 48- and 72-h exposures which are shown in Figure 4. For all values of our cell growth measurements, SMF effects became more visible at 72-h exposure.

Fibrosarcoma cells are adherent cells and grow attached to the bottom of the culture flask. The rate of cell growth depends on the orientation of the SMF with respect to the bottom of the flask that contains the cells. This observation can be seen in Figure 5, where the cellular response depends on both the orientation and intensity of the SMF applied. When the MF is oriented perpendicularly with respect to the bottom of the flask, the cell growth rate is higher for all applied MF intensities ($P < 0.01$ for 45 and 300 µT and $P < 0.001$ for 0.5, 100, 400, 500, and 600 µT) except

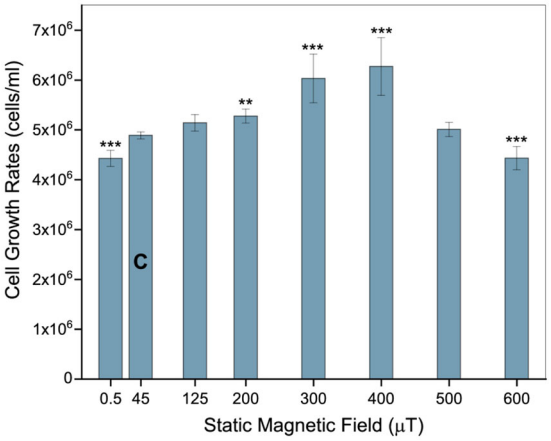


Fig. 3. Cell growth rates as a function of static magnetic field exposures between 0.5 and 600 µT with the fields perpendicular to the flask bottom. The data are expressed as mean ± SD; $n = 12$ for each group. C = control.

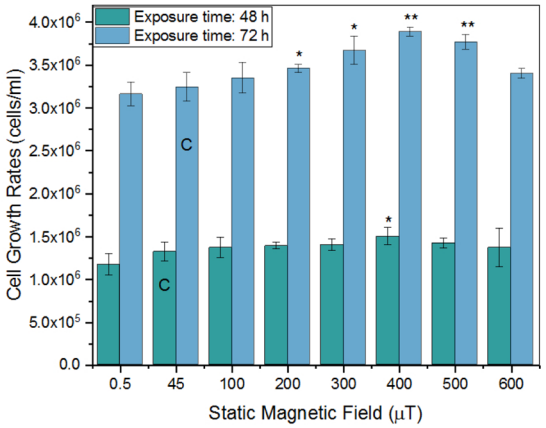


Fig. 4. Cell growth rates as a function of static magnetic field exposures for 48 and 72 h between 0.5 and 600 µT with the fields perpendicular to the flask bottom. The data are expressed as mean ± SD; $n = 12$ for each group. C = control.

1521186x, 2021, 3, Downloaded from https://onlinelibrary.wiley.com/doi/10.1002/bem.22332 by University Of Colorado Libraries, Wiley Online Library on [30/05/2024]. See the Terms and Conditions (https://onlinelibrary.wiley.com/terms-and-conditions) on Wiley Online Library for rules of use; OA articles are governed by the applicable Creative Commons License

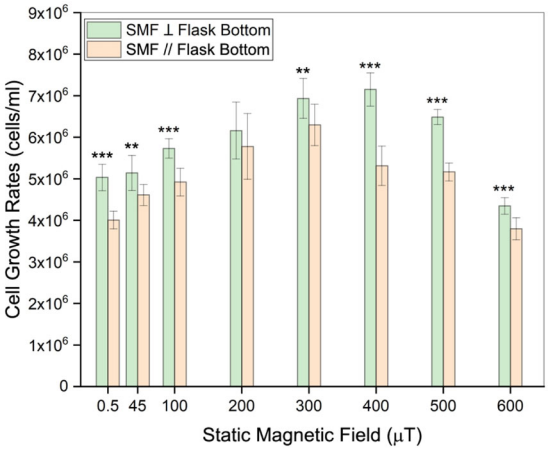


Fig. 5. Cell growth rates as a function of the orientation of static magnetic field with respect to the bottom of the flask. The data are expressed as mean ± SD; $n = 12$ for each group.

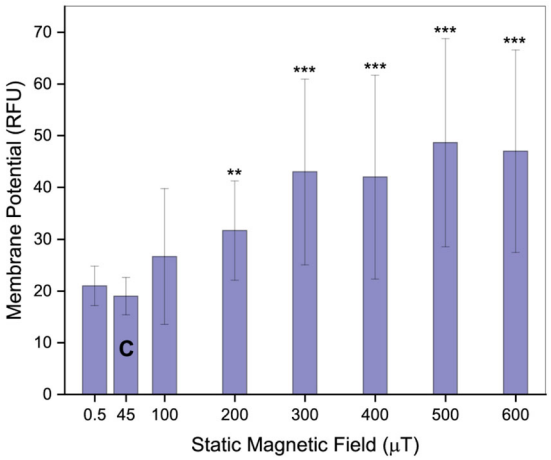


Fig. 6. Membrane potential as a function of static magnetic field exposure between 0.5 and 600 μT. An increase in relative fluorescence units (RFU) indicates reduction of the absolute value of negative membrane potential. The data are expressed as mean ± SD; $n = 63$ for each group. C = control.

for 200 μT, where no statistically significant differences are observed. These data are consistent with those in Figure 4, but the numbers are slightly different due to small variations in the initial cell sample size and passage number.

Changes in Membrane Potentials With Changes in SMFs

The membrane potential is created by the differences in ion concentrations between the inside and outside of the cell membrane and maintained by ion currents through ion channels and by ion transporters. Changes in membrane potential are caused by depolarization and hyperpolarization. Cellular excitations focus on depolarization of the membrane potential and associated changes in ionic equilibria across the cell membrane and offer a basis for an understanding of the first events in cell membrane electrochemical stimuli at the cell surface [Adey, 1988].

Human fibrosarcoma cells are stained with a FluoVolt Membrane Potential Kit (Thermo Fisher Scientific) to measure the response of membrane potential to exposed SMF. Depolarization of the cell membrane facilitates the marker′s entry and produces an increase in the intensity of the fluorescence. Figure 6 shows that membrane potential becomes less negative (lower absolute value) as we increase the MF. Significant differences are observed with respect to the control for 200 μT ($P < 0.01$) and for 300–600 μT ($P < 0.001$). Less negative values in membrane potentials below those observed for quiescent cells of the same time are typical of both growing cells and tumor cells [Levin, 2007].

Changes in Mitochondrial Calcium With Changes in SMFs

The ionic calcium concentrations are measurements of the active fraction of the stored calcium from the metabolic, physiological, and biochemical points of view. Efficient calcium signaling requires maintenance of calcium homeostasis, with basal cytosolic calcium concentrations kept low and stable by storage of calcium ions in the endoplasmic reticulum and in the mitochondria [Berridge et al., 2003].

Figure 7 shows that SMF induced an increase in mitochondrial calcium concentration with increasing MF.

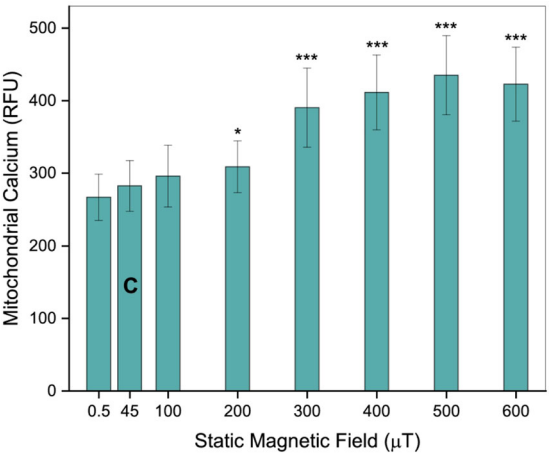


Fig. 7. Mitochondrial calcium concentrations as a function of static magnetic field for fields between 0.5 and 600 μT oriented at 90° with respect to the plane of the flask bottoms containing the cells. The data are expressed as mean ± SD; $n = 63$ for each group. C = control.

1521186x, 2021, 3, Downloaded from https://onlinelibrary.wiley.com/doi/10.1002/bem.22332 by University Of Colorado Libraries, Wiley Online Library on [30/05/2024]. See the Terms and Conditions (https://onlinelibrary.wiley.com/terms-and-conditions) on Wiley Online Library for rules of use; OA articles are governed by the applicable Creative Commons License

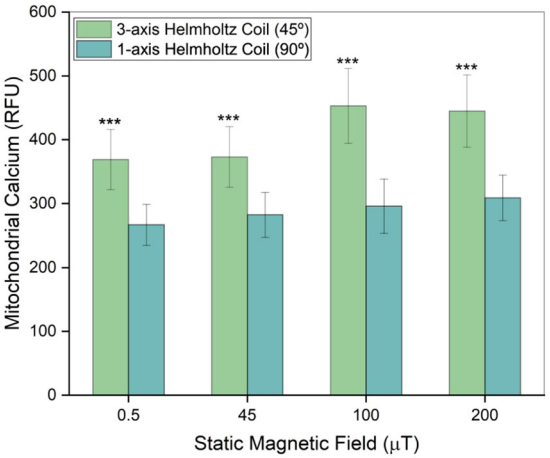


Fig. 8. Mitochondrial calcium concentrations as a function of static magnetic field for fields oriented at 45° and 90° with respect to the plane of the flask bottoms containing the cells. The data are expressed as mean ± SD; $n = 63$ for each group. The one-axis Helmholtz coil generated a magnetic field perpendicular to the bottom of the plate.

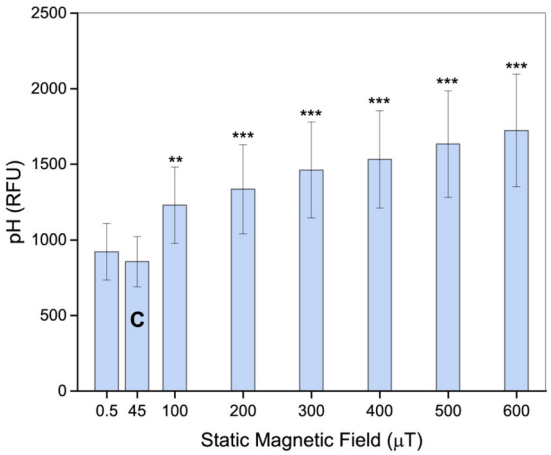


Fig. 9. Intracellular pH as a function of static magnetic field exposure between 0.5 and 600 μT. An increase in relative fluorescence units (RFU) indicates a decrease in intracellular pH. The data are expressed as mean ± SD; $n = 63$ for each group. C = control.

Significant differences are observed with respect to the control for 200 μT ($P < 0.05$) and for 300–600 μT ($P < 0.001$). In Figure 8, a separate set of measurements made with three-axis coils shows that the mitochondrial calcium concentration also depends on the orientation as well as the intensity of the SMF applied. Figure 8 shows mitochondrial calcium concentrations as a function of SMF for fields oriented at 45° and 90° with respect to the plane of the flask bottoms containing the cells. The data are expressed as mean ± SD; $n = 63$ for each group. The one-axis Helmholtz coil generated an MF perpendicular to the bottom of the plate.

Changes in Intracellular pH With Changes in SMFs

Intracellular pH or cytosolic pH is tightly regulated within cells. Imbalance in intracellular pH can affect many cellular functions, such as ionic homeostasis, ROS balance, apoptosis, cell cycle, and cellular mobility [Loiselle and Casey, 2010; Schulz and Münzel, 2011]. Figure 9 shows a decrease in pH when the intensity of the magnetic field increases. Cancer cells are known to acidify their environment and, consequently, the interior of the cells themselves is alkalized. It has been demonstrated that cancer cells proliferate less and in a less robust manner when their internal pH is lowered [Persi et al., 2018].

Changes in ROS With Changes in SMFs

ROS are molecules containing oxygen and are highly chemically reactive, including those featured in the measurements shown in Figures 10–13. ROS are a necessary biochemical component for the maintenance of healthy cells and tissues. However, in excess concentration, they can be highly cytotoxic, leading to cell and tissue damage. Substantial evidence now shows that the imbalance between the production of ROS and antioxidant defense mechanisms in the tissues can be linked to exposure to electromagnetic fields [Morabito et al., 2010; Çiğ and Nazıroğlu, 2015].

Changes in Oxidative Stress With Changes in SMFs

Oxidative Stress is the imbalance between the production of pro-oxidants and antioxidants. Reactive oxygen and nitrogen species can be used as messengers in normal cell functions. However, at oxidative stress levels, they can disrupt normal physiological pathways and cause cell death [Kushnareva et al., 2002]. CellROX Green only becomes fluorescent with subsequent binding to DNA, limiting its presence to the nucleus or mitochondria. Our results indicate that oxidative stress increases significantly for 100 and 200 μT ($P < 0.001$) and moderately for 400 μT ($P < 0.05$). There are no significant differences with respect to the control for the other values of the applied MF. That is, there is a balance between the production of pro-oxidants and antioxidants (Fig. 10).

Changes in Hydrogen Peroxide With Changes in SMFs

The concentration of H_2O_2 in the cells varies greatly, from 1 nM to 100 μM, depending on the organism or tissue. H_2O_2 has been implicated in the

1521186x, 2021, 3, Downloaded from https://onlinelibrary.wiley.com/doi/10.1002/bem.22332 by University Of Colorado Libraries, Wiley Online Library on [30/05/2024]. See the Terms and Conditions (https://onlinelibrary.wiley.com/terms-and-conditions) on Wiley Online Library for rules of use; OA articles are governed by the applicable Creative Commons License

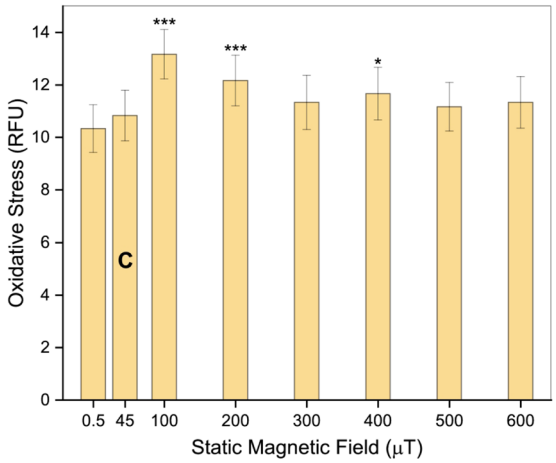


Fig. 10. Oxidative Stress as a function of static magnetic field exposure between 0.5 and 600 μT. The data are expressed as mean ± SD; $n = 63$ for each group. C = control.

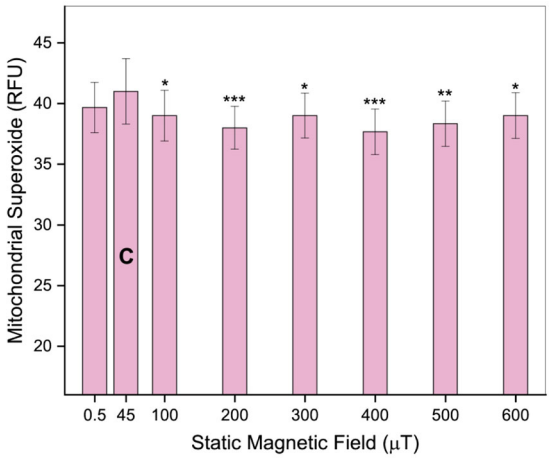


Fig. 12. Mitochondrial superoxide concentrations as a function of static magnetic field exposure between 0.5 and 600 μT. The data are expressed as mean ± SD; $n = 63$ for each group. C = control.

redox regulation of several physiological processes, including signal transduction, response to oxidative stress, development, cell proliferation, and apoptosis [Halliwell and Gutteridge, 2006]. The concentrations of H_2O_2 show a non-linear response as a function of the applied MF′s intensity. For 100, 200, 500, and 600 μT, the concentration of H_2O_2 is higher than in the control ($P < 0.001$), and for 300 μT it is lower than in the control ($P < 0.05$). It is known that different concentrations of H_2O_2 activate different redox switches, which are key players in the regulation of biological pathways [Antunes and Brito, 2017].

Changes in Mitochondrial Superoxide With Changes in SMFs

Mitochondrial superoxide is generated as a byproduct of oxidative phosphorylation. In an otherwise tightly coupled electron transport chain, approximately 1–3% of mitochondrial oxygen consumed is incompletely reduced; those "leaky" electrons can quickly interact with molecular oxygen to form superoxide anions, O_2^-, the predominant ROS in mitochondria [Droge, 2002].

We observed that mitochondrial superoxide production decreased with exposure to MF (Fig. 12).

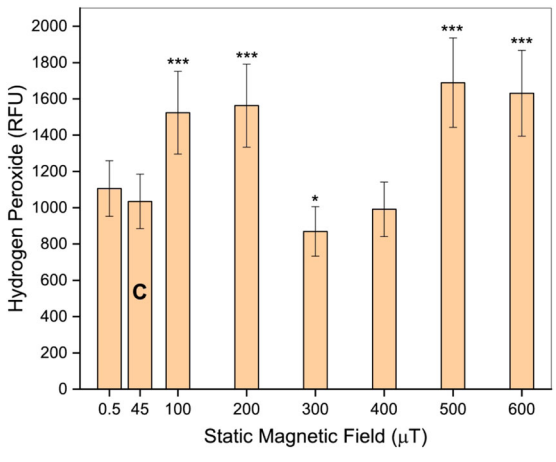


Fig. 11. Hydrogen peroxide concentrations as a function of static magnetic field exposure between 0.5 and 600 μT. The data are expressed as mean ± SD; $n = 63$ for each group. C = control.

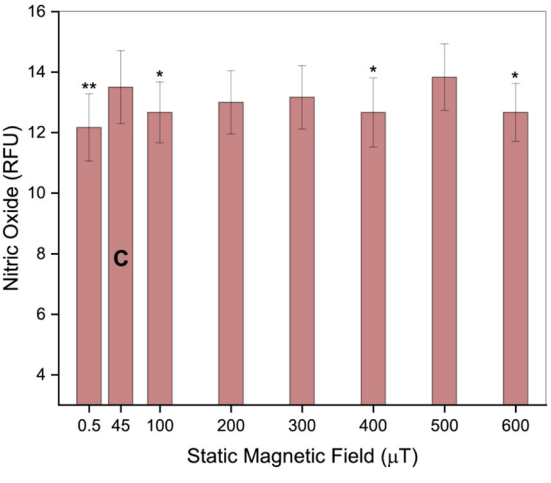


Fig. 13. Nitric oxide concentration as a function of static magnetic field exposure between 0.5 and 600 μT. The data are expressed as mean ± SD; $n = 63$ for each group. C = control.

1521186x, 2021, 3, Downloaded from https://onlinelibrary.wiley.com/doi/10.1002/bem.22332 by University Of Colorado Libraries, Wiley Online Library on [30/05/2024]. See the Terms and Conditions (https://onlinelibrary.wiley.com/terms-and-conditions) on Wiley Online Library for rules of use; OA articles are governed by the applicable Creative Commons License

Significant differences are observed with respect to the control for 100, 300, and 600 μT ($P < 0.05$); for 500 μT ($P < 0.01$); and for 200 and 400 μT ($P < 0.001$).

Changes in Nitric Oxide With Changes in SMFs

NO has a magnetic dipole moment and is a free radical. It was not until recently that beneficial roles for NO were discovered in biological systems. Further work has shown that NO is a ubiquitous messenger in the cardiovascular, immune, and nervous systems [Geddes and Lakowicz, 2007]. DAF-FM diacetate is cell-permeant and passively diffuses across cellular membrane. In Figure 13 we can see that NO decreases with respect to the control for 0.5 μT ($p < 0.01$); and for 100, 400, and 600 μT ($P < 0.05$). Other studies have reported that exposure to SMFs produces a decrease in NO levels and in other parameters that characterize cell stress [Coballase-Urrutia et al., 2018].

SUMMARY AND DISCUSSION

We observed both acceleration and inhibition of the growth rates when HT-1080 cells were exposed to SMFs between 0.5 and 600 μT. Acceleration of cell growth is seen between 200 and 400 μT and decreases are seen at 0.5 and 600 μT along with variations in the membrane potentials, mitochondrial calcium, ROS, superoxide (O_2^-), NO, H_2O_2, intercellular pH, and oxidative stress.

Mitochondria are at the center of many diverse cellular functions as integrators of signals between the organelle and the nucleus [Karu, 2008]. And oxidative phosphorylation in mitochondria provides most of the ATP in nearly all cell types [Griffiths and Rutter, 2009]. This produced energy is stored as an electrochemical gradient, which comprises the pH gradient and the membrane potential. There appears to be multifactor crosstalk among Ca^{2+}, electrochemical gradient, and ROS. It is also known that the uncoupling of oxidative phosphorylation and ATP synthesis not only changes the electrochemical gradient but also affects mitochondrial calcium accumulation and ROS generation [Brookes et al., 2004]. Therefore, mitochondrial Ca^{2+} have a key role in the regulation of energy supply and demand. Charged species, particularly calcium ions, are essential in the regulation of the plasma membrane potential. The cell membrane is often considered as the main target for MFs, and it has been suggested that even a small change in transmembrane voltage could trigger a significant modulation of cell function [Markov, 2007].

In our experiments, the amplitudes of mitochondrial calcium responses increased with the SMF strength. These results corroborate previous studies showing an increase in intracellular Ca^{2+} concentrations in several cell types after exposure to SMFs [Teodori et al., 2002; Dini and Abbro, 2005]. Bekhite et al. [2013] observed that depleting Ca^{2+} in the extracellular medium completely inhibited the SMF-induced [Ca^{2+}] signal. This provides strong evidence that Ca^{2+} influx across the plasma membrane is the mechanism responsible for the observed [Ca^{2+}] increase.

When calcium levels increase in cells, the activity of sodium-calcium exchangers and other specific ATP-dependent transporters increase to force out calcium ions. As a result, cells under SMF exposure require more ATP energy for maintaining calcium homeostasis. This not only affects intracellular calcium signaling, but cellular metabolism may be directly changed. This change can be explained by the increase in the metabolic rate. Of the parameters measured, intracellular pH, mitochondrial calcium, membrane potential, and cell growth clearly showed this relationship with exposure to SMFs. Overall, intracellular pH decreased while the magnitude of the membrane potential, mitochondrial calcium, and cell growth increased with the intensity of SMFs. This effect was observed for cell growth from 0.5 to 400 μT and for mitochondrial calcium from 0.5 to 500 μT. It was also found that the responses of cell growth rates and mitochondrial calcium concentrations depend on the orientation of SMF with respect to the bottom of the flask.

In the present study, we looked at mitochondrial ROS generation as an important source for ROS signaling and concentrated our attention on the initial parts of the mitochondrial signaling pathways. Mitochondrial superoxide, H_2O_2, and NO are considered important intra-mitochondrial signaling molecules. In our experiments, ROS responses to the SMF were more complex. Changes in H_2O_2 are not linearly correlated with cell growth. This might be due to increases in antioxidant concentrations [Rosenspire et al., 2005]. Decreases in H_2O_2 correspond to where we observed the highest increase in cell growth rates. There are various studies showing that low levels of H_2O_2 can initiate cell proliferation [Antunes and Brito, 2017; Sies, 2017]. The mitochondrial superoxide and the NO tend to decrease with the increase in MF. The mitochondrial superoxide decreased with respect to the control for all SMF values, being highly significant for 200 and 400 μT, and the NO decreased with respect to the control for 0.5, 100, 400, and 600 μT. H_2O_2 and oxidative stress tend to increase

1521186x, 2021, 3, Downloaded from https://onlinelibrary.wiley.com/doi/10.1002/bem.22332 by University Of Colorado Libraries, Wiley Online Library on [30/05/2024]. See the Terms and Conditions (https://onlinelibrary.wiley.com/terms-and-conditions) on Wiley Online Library for rules of use; OA articles are governed by the applicable Creative Commons License

with the increase in SMF. In both parameters, a highly significant increase was observed for 100 and 200 μT.

The importance of these results is that variations of background MFs can both increase and decrease cell growth rates and corresponding concentrations of ROS and other signaling molecules. These observed changes are significant as different concentration levels of ROS could have beneficial or adverse effects on biology. In conclusion, the basic effect observed here is that changes in SMFs create a change in the growth rate of the cells and changes in some important molecular concentrations on both sides of the cell and mitochondrial membrane. Though the growth rate is one of the parameters that we have studied, the changes in the signaling molecules and other cell parameters might cause long-term effects in biological systems. An example of this is long-term changes in oxidative stress related to cancer and aging-related diseases. Canceling out the earth′s MF substantially, down to 0.5 μT by Mu metal cages, not only gave us the capability to eliminate background noise but also allowed us to observe effects at a level much lower than the earth′s MF. Thus, in this study, we believe that measuring and controlling the SMFs and eliminating the effects of temperature and background noise in experiments are important for attempting to understand the effects of electromagnetic fields on biological systems. Additionally, we believe that the amplitude, angle of incidence, and length of the exposure can lead to variable results and need to be included in the description of experimental protocols [Barnes and Greenebaum, 2015].

Future work will include time-varying MFs, where we expect to see both electric and MF effects. Time-varying MFs induce electric fields; other data indicate that both electric and MFs can induce changes in cell growth rates and other biological parameters [Bingham, 1996]. More research work will be required to determine the mechanisms by which these two different fields modify the behavior of cells.

ACKNOWLEDGMENTS

We greatly appreciate the contributions of Professor Mark Hernandez for supporting us with the equipment and lab space to carry out these experiments.

REFERENCES

Adey WR. 1988. Cell membranes: The electromagnetic environment and cancer promotion. Neurochem Res 13:671–677.

Antunes F, Brito PM. 2017. Quantitative biology of hydrogen peroxide signaling. Redox Biol 13:1–7.

Antunes F, Cadenas E. 2000. Estimation of H_2O_2 gradients across biomembranes. FEBS Lett 475:121–126.

Barnes FS, Greenebaum B. 2015. The effects of weak magnetic fields on radical pairs. Bioelectromagnetics 36:45–54.

Batchelor SN, Kay CWM, McLauchlan KA, Shkrob IA. 1993. Time-resolved and modulation methods in the study of the effects of magnetic fields on the yields of free-radical reactions. J Phys Chem 97:13250–13258.

Bekhite MM, Figulla HR, Sauer H, Wartenberg M. 2013. Static magnetic fields increase cardiomyocyte differentiation of *Flk*-1$^+$ cells derived from mouse embryonic stem cells via Ca^{2+} influx and ROS production. Int J Cardiol 167:798–808.

Belton M, Commerford K, Hall J, Prato FS, Carson JJL. 2008. Real-time measurement of cytosolic free calcium concentration in HL-60 cells during static magnetic field exposure and activation by ATP. Bioelectromagnetics 29:439–446.

Bernabò N, Saponaro I, Tettamanti E, Mattioli M, Barboni B. 2014. Acute exposure to a 2 mT static magnetic field affects ionic homeostasis of in vitro grown porcine granulosa cells. Bioelectromagnetics 35:231–234.

Berridge MJ, Bootman MD, Roderick HL. 2003. Calcium: calcium signalling: Dynamics, homeostasis and remodelling. Nat Rev Mol Cell Biol 4:517–529.

Bingham C. 1996. The effects of DC and ELF AC magnetic fields on the division rate of mastocytoma cells [PhD thesis]. Boulder, CO: University of Colorado Boulder.

Brookes PS, Yoon Y, Robotham JL, Anders MW, Sheu SS. 2004. Calcium, ATP, and ROS: A mitochondrial love-hate triangle. Am J Physiol Cell Physiol 287:C817–C833.

Calabrò E, Condello S, Currò M, Ferlazzo N, Caccamo D, Magazù S, Ientile R. 2013. Effects of low intensity static magnetic field on FTIR spectra and ROS production in SH-SY5Y neuronal-like cells. Bioelectromagnetics 34:618–629.

Çiğ B, Nazıroğlu M. 2015. Investigation of the effects of distance from sources on apoptosis, oxidative stress and cytosolic calcium accumulation via TRPV1 channels induced by mobile phones and Wi-Fi in breast cancer cells. Biochim Biophys Acta 1848:2756–2765.

Coballase-Urrutia E, Navarro L, Ortiz JL, Verdugo-Díaz L, Gallardo JM, Hernández ME, Estrada-Rojo F. 2018. Static magnetic fields modulate the response of different oxidative stress markers in a restraint stress model animal. BioMed Res Int 39:604–608.

Dini L, Abbro L. 2005. Bioeffects of moderate-intensity static magnetic fields on cell cultures. Micron 36:195–217.

Diwanji N, Bergmann A. 2018. An unexpected friend—ROS in apoptosis-induced compensatory proliferation: Implications for regeneration and cancer. Semin Cell Dev Biol 80:74–82.

Droge W. 2002. Free radicals in the physiological control of cell function. Physiol Rev 82:47–95.

Fanelli C, Coppola S, Barone R, Colussi C, Gualandi G, Volpe P, Ghibelli L. 1999. Magnetic fields increase cell survival by inhibiting apoptosis via modulation of Ca^{2+} influx. FASEB J 13:95–102.

Geddes CD, Lakowicz JR. 2007. Advanced Concepts in Fluorescence Sensing: Part A: Small Molecule Sensing (Vol. 9). Norwell, MA: Springer Science & Business Media. p. 163.

Ghodbane S, Lahbib A, Sakly M, Abdelmelek H. 2013. Bioeffects of static magnetic fields: Oxidative stress, genotoxic effects, and cancer studies. BioMed Res Int: 602987. 2013:1–12.

Gorrini C, Harris IS, Mak TW. 2013. Modulation of oxidative stress as an anticancer strategy. Nat Rev Drug Discov 12:931–947.

1521186x, 2021, 3, Downloaded from https://onlinelibrary.wiley.com/doi/10.1002/bem.22332 by University Of Colorado Libraries, Wiley Online Library on [30/05/2024]. See the Terms and Conditions (https://onlinelibrary.wiley.com/terms-and-conditions) on Wiley Online Library for rules of use; OA articles are governed by the applicable Creative Commons License

Greenebaum B, Mild KH. 2018. Environmental and occupational DC and low frequency electromagnetic fields. In: Greenebaum B, Barnes F, editors. Bioengineering and Biophysical Aspects of Electromagnetic Fields, Fourth Edition. Boca Raton, FL: CRC Press. pp 29–53.

Griffiths EJ, Rutter GA. 2009. Mitochondrial calcium as a key regulator of mitochondrial ATP production in mammalian cells. Biochim Biophys Acta 1787:1324–1333.

Grissom CB. 1995. Magnetic field effects in biology: A survey of possible mechanisms with emphasis on radical-pair recombination. Chem Rev 95:3–24.

Halliwell B, Gutteridge JM. 2006. Free Radicals in Biology and Medicine. New York, NY: Oxford University Press. p. 190.

Hancock JT, Desikan R, Neill SJ. 2001. Role of reactive oxygen species in cell signalling pathways. Biochem Soc Trans 29:345–350.

Hayashi H. 2004. Introduction to Dynamic Spin Chemistry: Magnetic Field Effects on Chemical and Biochemical Reactions. Singapore: World Scientific Publishing Co. p. 21.

Jouni FJ, Abdolmaleki P and Movahedin M. 2013. Investigation on the effect of static magnetic field up to 15 mT on the viability and proliferation rate of rat bone marrow stem cells. In Vitro Cellular & Developmental Biology-Animal 49:212–219.

Karu TI. 2008. Mitochondrial signaling in mammalian cells activated by red and near-IR radiation. Photochem Photobiol 84:1091–1099.

Kim EC, Leesungbok R, Lee SW, Lee HW, Park SH, Mah SJ, Ahn SJ. 2015. Effects of moderate intensity static magnetic fields on human bone marrow-derived mesenchymal stem cells. Bioelectromagnetics 36:267–276.

Kushnareva Y, Murphy AN, Andreyev A. 2002. Complex I-mediated reactive oxygen species generation: Modulation by cytochrome c and $NAD(P)^+$ oxidation–reduction state. Biochem J 368:545–553.

Levin M. 2007. Large-scale biophysics: Ion flows and regeneration. Trends Cell Biol 17:261–270.

Liboff AR. 2007. The ion cyclotron resonance hypothesis. In: Barnes FS, Greenebaum B, editors. Bioengineering and Biophysical Aspects of Electromagnetic Fields. Boca Raton, FL: CRC Press. pp 261–292.

Loiselle FB, Casey JR. 2010. Measurement of intracellular pH. Methods Mol Biol 637:311–331.

Markov MS. 2007. Magnetic field therapy: A review. Electromagn Biol Med 26:1–23.

Moloney JN, Cotter TG. 2018. ROS signalling in the biology of cancer. Semin Cell Dev Biol 80:50–64.

Morabito C, Rovetta F, Bizzarri M, Mazzoleni G, Fanò G, Mariggiò MA. 2010. Modulation of redox status and calcium handling by extremely low frequency electromagnetic fields in C2C12 muscle cells: A real-time, single-cell approach. Free Radic Biol Med 48:579–589.

Morris CE, Skalak TC. 2008. Acute exposure to a moderate strength static magnetic field reduces edema formation in rats. Am J Physiol Heart Circ Physiol 294:H50–H57.

Novikov V, Yablokova E, Shaev I and Fesenko E. 2020. The Effect of a Weak Static Magnetic Field in the Range of Magnitudes from "Zero" Field (0.01 μT) to 100 μT on the Production of Reactive Oxygen Species in Nonactivated Neutrophils Biophysics 65:443–447.

Persi E, Duran-Frigola M, Damaghi M, Roush WR, Aloy P, Cleveland JL, Gillies RJ, Ruppin E. 2018. Systems analysis of intracellular pH vulnerabilities for cancer therapy. Nat Commun 9:2997.

Portelli L, Schomay T, Barnes F. 2013. Inhomogeneous background magnetic field in biological incubators is a potential confounder for experimental variability and reproducibility. Bioelectromagnetics 34:337–348.

Prina-Mello A, Campbell V, Coey J. 2005. Static magnetic field effects on cells. A possible road to cell differentiation. NSTI-Nanotech 1:96–99.

Reczek CR, Chandel NS. 2017. The two faces of reactive oxygen species in cancer. Annu Rev Cancer Biol 1:79–98.

Rosenspire AJ, Kindzelskii AL, Simon BJ, Petty HR. 2005. Real-time control of neutrophil metabolism by very weak ultra-low frequency pulsed magnetic fields. Biophys J 88:3334–3347.

Schulz E, Münzel T. 2011. Intracellular pH: A fundamental modulator of vascular function. Circulation 124:1806–1807.

Sies H. 2017. Hydrogen peroxide as a central redox signaling molecule in physiological oxidative stress: Oxidative eustress. Redox Biol 11:613–619.

Surma SV, Belostotskaya GB, Shchegolev BF, Stefanov VE. 2014. Effect of weak static magnetic fields on the development of cultured skeletal muscle cells. Bioelectromagnetics 35:537–546.

Sullivan K, Balin AK and Allen RG. 2011. Effects of static magnetic fields on the growth of various types of human cells. Bioelectromagnetics 32:140–147.

Teodori L, Göhde W, Valente MG, Tagliaferri F, Coletti D, Perniconi B, Bergamaschi A, Cerella C, Ghibelli L. 2002. Static magnetic fields affect calcium fluxes and inhibit stress-induced apoptosis in human glioblastoma cells. Cytometry 49:143–149.

Timmel C, Henbest K. 2004. A study of spin chemistry in weak magnetic fields. Phil Trans R Soc London Ser A 362:2573–2589.

Timmel CR, Till U, Brocklehurst B, Mclauchlan KA, Hore PJ. 1998. Effects of weak magnetic fields on free radical recombination reactions. Mol Phys 95:71–89.

Turrens JF. 2003. Mitochondrial formation of reactive oxygen species. J Physiol 552:335–344.

Van Huizen A, Morton J, Kinsey L, Von Kannon D, Saad M, Birkholz T, Czajka J, Cyrus J, Barnes F, Beane W. 2019. Weak magnetic fields alter stem cell-mediated growth. Sci Adv 5:eaau7201.

Vriz S, Reiter S, Galliot B. 2014. Cell death: A program to regenerate. Curr Top Dev Biol 108:121–151.

Wang H, Zhang X. 2017. Magnetic fields and reactive oxygen species. Int J Mol Sci 18:2175.

Zhang J, Wang X, Vikash V, Ye Q, Wu D, Liu Y, Dong W. 2016. ROS and ROS-mediated cellular signaling. Oxid Med Cell Longev:4350965.

1521186x, 2021, 3, Downloaded from https://onlinelibrary.wiley.com/doi/10.1002/bem.22332 by University Of Colorado Libraries, Wiley Online Library on [30/05/2024]. See the Terms and Conditions (https://onlinelibrary.wiley.com/terms-and-conditions) on Wiley Online Library for rules of use; OA articles are governed by the applicable Creative Commons License